

Novel Organotellurium(IV) Diazides and Triazides[#]

Thomas M. Klapötke,* Burkhard Krumm, Peter Mayer,[†] Holger Piotrowski,[†] Oliver P. Ruscitti, and Alexander Schiller

Department of Chemistry, Ludwig-Maximilians University of Munich, Butenandtstrasse 5-13 (D), D-81377 Munich, Germany

Received October 2, 2001

New series dialkyltellurium(IV) diazides $R_2Te(N_3)_2$ ($R = CH_3$ (6), C_2H_5 (7), $n-C_3H_7$ (8), $i-C_3H_7$ (9), $c-C_6H_{11}$ (10)) and alkyl/aryl tellurium(IV) triazides $R'Te(N_3)_3$ ($R' = CH_3$ (11), C_2H_5 (12), $n-C_3H_7$ (13), $i-C_3H_7$ (14), C_6H_5 (15), 2,4,6-($CH_3)_3C_6H_2$ (16)) were synthesized by the straightforward substitution of fluorine atoms in the corresponding tellurium difluorides, or trifluorides respectively, with trimethylsilyl azide. In addition to standard characterization methods, the first crystal structures of covalent organotellurium(IV) triazides 12, 13, 14, and 16 have been determined. Ethyltellurium(IV) triazide, $C_2H_5Te(N_3)_3$ (12), crystallizes in the monoclinic space group $P2_1/n$, $a = 8.4530(2)$ Å, $b = 7.9094(2)$ Å, $c = 12.6288(3)$ Å, $\beta = 91.876(1)$ °. n -Propyltellurium(IV) triazide, $n-C_3H_7Te(N_3)_3$ (13), crystallizes in the monoclinic space group $P2_1/n$ as well, $a = 8.7999(2)$ Å, $b = 7.9674(2)$ Å, $c = 13.2334(3)$ Å, $\beta = 94.626(1)$ °. Isopropyltellurium(IV) triazide, $i-C_3H_7Te(N_3)_3$ (14), crystallizes in the monoclinic space group $C2/c$, $a = 20.058(2)$ Å, $b = 6.9620(3)$ Å, $c = 15.030(1)$ Å, $\beta = 114.260(9)$ °. Mesityltellurium(IV) triazide, 2,4,6-($CH_3)_3C_6H_2Te(N_3)_3$ (16), crystallizes monoclinic as well; the space group is $P2_1/c$, $a = 7.5503(6)$ Å, $b = 23.581(1)$ Å, $c = 7.5094(6)$ Å, $\beta = 91.295(9)$ °. The structures and vibrational frequencies of the methyl derivatives dimethyltellurium(IV) diazide (6) and methyltellurium(IV) triazide (11) have been calculated by density functional theory methods and were compared with the experimental metric parameters and vibrational data.

Introduction

The number of nitrogen compounds containing a direct chalcogen–nitrogen bond is enormous, but few selenium and tellurium nitrogen species have been isolated, in comparison with the number of sulfur–nitrogen compounds¹ (e.g., the best known is S_4N_4 ²). The binary nitrogen compounds of selenium and tellurium are rare and include the well-known Se_4N_4 ,³ Te_4N_4 ,⁴ and Te_3N_4 ,⁵ which have been only ambiguously identified, and the complex tellurium nitride $[Te_6N_8 \cdot (TeCl_4)]$.⁶ The first tellurium azides were synthesized by

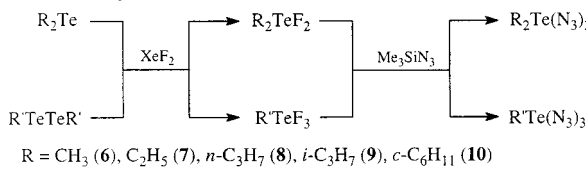
reacting $TeCl_4$ with Me_3SiN_3 ; the resulting compounds $TeCl_3N_3$ and $TeCl_2(N_3)_2$ were reported to be explosive solids.⁷ The first ionic binary tellurium azide, $[Te(N_3)_3] \cdot [SbF_6]$, was prepared from $Te_4(SbF_6)_2$ and KN_3 and structurally characterized.⁸ Not only was this the first binary chalcogen–nitrogen compound, but also one further example of binary main-group element cations. However, only a few tellurium azides are known in the literature,^{9–11} and only two, $[Te(N_3)_3][SbF_6]$ and $[(C_6H_5)_2TeN_3]_2O$, have been structurally characterized using X-ray diffraction techniques. Recently, we communicated a general and easy route to covalent diaryltellurium(IV) diazides along with structural characterization of $(C_6H_5)_2Te(N_3)_2$ and $(C_6F_5)_2Te(N_3)_2$.¹²

[#] Dedicated to Professor Wolfgang Beck on the occasion of his 70th birthday.

* To whom correspondence should be addressed. Fax: +49-89-2180-7492. E-mail: thomas.m.klapoetke@cup.uni-muenchen.de.

[†] X-ray structure determination.

- (1) Schmidt, M.; Siebert, W. *Comp. Inorg. Chem.* **1973**, 2, 898.
- (2) DeLucia, M. L.; Coppens, P. *Inorg. Chem.* **1978**, 17, 2336.
- (3) (a) Bärnighausen, H.; von Volkmann, T.; Jander, J. *Acta Crystallogr. 1966*, 21, 571. (b) Folkerts, H.; Neumüller, B.; Dehnice, K. Z. *Anorg. Allg. Chem.* **1994**, 620, 1011.
- (4) Garcia-Fernandez, H. *Bull. Soc. Chim. Fr.* **1973**, 1210.
- (5) Schmitz-Dumont, O.; Ross, B. *Angew. Chem., Int. Ed. Engl.* **1967**, 6, 1071.
- (6) Massa, W.; Lau, C.; Möhlen, M.; Neumüller, B.; Dehnice, K. *Angew. Chem., Int. Ed.* **1998**, 37, 2840.
- (7) Wiberg, N.; Schwenk, G.; Schmid K. H. *Chem. Ber.* **1972**, 105, 1209.
- (8) Johnson, J. P.; MacLean, G. K.; Passmore, J.; White, P. S. *Can. J. Chem.* **1989**, 67, 1687.
- (9) (a) Klapötke, T. M. *Chem. Ber.* **1997**, 130, 443. (b) Tornieporth-Oetting, I. C.; Klapötke, T. M. *Angew. Chem., Int. Ed. Engl.* **1995**, 34, 511.
- (10) Magnus, P.; Roe, M. B.; Lynch, V.; Hulme, C. *J. Chem. Soc., Chem. Commun.* **1995**, 1609.
- (11) (a) Fimm, W.; Sladky, F. *Chem. Ber.* **1991**, 124, 1131. (b) Gorell, I. B.; Ludman C. J.; Matthews, R. S. *J. Chem. Soc., Dalton Trans.* **1992**, 2899.

Scheme 1. Synthesis of Tellurium(IV) Di- and Triazides

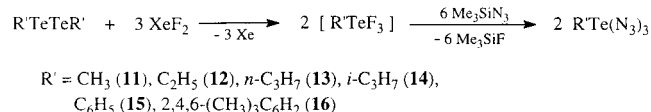
Investigations on selenium azides have provided the first evidence for their existence in solution by low-temperature NMR spectroscopy.¹³ In contrast, sulfur azides are relatively well-known, with sulfonyl diazide, $\text{SO}_2(\text{N}_3)_2$,¹⁴ being one of the simplest examples of an inorganic chalcogen diazide and $\text{C}_6\text{H}_5\text{S}(\text{O})\text{N}_3$ ¹⁵ as one of a variety of organic derivatives. In this paper we present our progress in tellurium(IV) azide chemistry with the first dialkyltellurium(IV) diazides and the synthesis and properties of novel covalent tellurium(IV) triazides.

Results and Discussion

The synthetic strategy used is closely related to the preparation of $(\text{C}_6\text{H}_5)_2\text{Te}(\text{N}_3)_2$ and $(\text{C}_6\text{F}_5)_2\text{Te}(\text{N}_3)_2$.¹² The starting materials, diorgano tellurides and diorgano ditellurides, were obtained by literature methods.^{16–19} These were then oxidized with xenon difluoride to form the corresponding diorganotellurium difluorides and organotellurium trifluorides. The trifluorides were not isolated and were treated with a slight excess of trimethylsilyl azide, resulting in the formation of the desired compounds according to Scheme 1.

Although TeCl_3N_3 and $\text{TeCl}_2(\text{N}_3)_2$ were prepared by substitution of chlorine atoms in TeCl_4 with trimethylsilyl azide,⁷ diorganotellurium(IV) dichlorides R_2TeCl_2 or dibromides R_2TeBr_2 , as well as the corresponding organotellurium(IV) trichlorides RTeCl_3 or tribromides RTeBr_3 , did not react with trimethylsilyl azide. The relatively low bond enthalpy (298 K) of $\text{Si}-\text{Br}$ (329 kJ mol^{-1}) and $\text{Si}-\text{Cl}$ (398 kJ mol^{-1}) bonds compared with $\text{Si}-\text{F}$ (595 kJ mol^{-1}) of the byproduct Me_3SiHal ($\text{Hal} = \text{Br}$, Cl , or F) does not account for the observed reactivity trends. Either kinetic effects or each organic substituent affects and varies the electronic state of tellurium in $\text{R}_2\text{TeCl}_2/\text{R}_2\text{TeBr}_2$ and $\text{RTeCl}_3/\text{RTeBr}_3$ to such an extent that no substitution of the chlorine or bromine atoms occurs.

- (12) Klapötke, T. M.; Krumm, B.; Mayer, P.; Ruscitti, O. P. *Inorg. Chem.* **2000**, *39*, 5426.
- (13) Klapötke, T. M.; Krumm, B.; Mayer, P.; Polborn, K.; Ruscitti, O. P. *Phosphorus, Sulfur, Silicon Relat. Elem.* **2001**, *172*, 119.
- (14) Nojima, M. *J. Chem. Soc., Perkin Trans. 1* **1979**, 1811 and references therein.
- (15) Maricich, T. J.; Hoffman, V. L. *J. Am. Chem. Soc.* **1974**, *96*, 7770.
- (16) (a) Bhasin, K. K.; Gupta, V.; Gantam, A.; Sharma, R. P. *Synth. Commun.* **1990**, *20*, 2191. (b) Chen, M. T.; George, J. W. *J. Organomet. Chem.* **1968**, *12*, 401.
- (17) Aso, Y.; Yamashita, H.; Otsubo, T.; Ogura, F. *J. Org. Chem.* **1989**, *54*, 5627.
- (18) Akiba, M.; Lakshminathan, M. V.; Jen, K.; Cava, M. P. *J. Org. Chem.* **1984**, *49*, 4819.
- (19) Karaghiosoff, K.; Klapötke, T. M.; Krumm, B.; Ruscitti, O. P. *J. Organomet. Chem.* **1999**, *577*, 69.

Scheme 2. Stoichiometry for the Preparation of the Alkyl and Aryltellurium(IV) Triazides

Dialkyltellurium(IV) Diazides $\text{R}_2\text{Te}(\text{N}_3)_2$. The precursors of the dialkyltellurium(IV) diazides, R_2TeF_2 , were synthesized by reacting equimolar amounts of xenon difluoride with the dialkyl tellurides in dichloromethane solution at -50°C . Only minimal spectroscopic data exist for $(\text{CH}_3)_2\text{TeF}_2$ (**1**),²⁰ the higher dialkyltellurium(IV) difluorides have not been reported ($\text{R} = \text{C}_2\text{H}_5$ (**2**), $n\text{-C}_3\text{H}_7$ (**3**), $i\text{-C}_3\text{H}_7$ (**4**), $c\text{-C}_6\text{H}_{11}$ (**5**)) and are therefore fully characterized in this work for the first time.

The reaction of dialkyltellurium(IV) difluorides R_2TeF_2 **1–5** with stoichiometric amounts of trimethylsilyl azide (Scheme 1) in dichloromethane at 0°C resulted in the formation of the corresponding tellurium(IV) diazides. The byproduct trimethylsilyl fluoride was detected by ^{19}F NMR spectroscopy.

The diazides **6–9** are colorless liquids (solid **10**) which explode when heated in a flame, contrasting with $(\text{C}_6\text{H}_5)_2\text{Te}(\text{N}_3)_2$ and $(\text{C}_6\text{F}_5)_2\text{Te}(\text{N}_3)_2$, which are colorless and non-explosive solids.¹² All diazides described are moderately soluble in common organic solvents and hydrolyze slowly in air, and moisture promotes their decomposition with formation of HN_3 .

Alkyl/Aryltellurium(IV) Triazides $\text{R}'\text{Te}(\text{N}_3)_3$. The Te–Te bond (dissociation energy 126 kJ mol^{-1})²¹ in diorgano ditellurides is cleaved oxidatively with xenon difluoride to form the corresponding organotellurium(IV) trifluorides $\text{R}'\text{TeF}_3$, which show extreme moisture sensitivity in glass vessels. Therefore, they were generated in situ and converted to the organotellurium(IV) triazides by reaction with the azide moiety (Scheme 2).

The triazides **11–16** were isolated as colorless (pale yellow **16**) solids. Their solubility is less in common organic solvents when compared with the corresponding diazides, but increases with increasing aliphatic content. Tellurium(IV) triazides hydrolyze in air, and again, moisture promotes decomposition with formation of HN_3 , which is detected by ^{14}N NMR spectroscopy. Explosion occurs with a blue flash upon contact with a flame; the aryl derivatives **15** and **16** form intense smoke. In general, no shock or impact sensitivity was observed.²² The triazidotellurium cation is believed to be nonexplosive; however, explosions occurred with byproducts and impurities.⁸ Methyltellurium(IV) triazide (**11**) is the most nitrogen rich neutral tellurium compound reported so far, with a nitrogen content of 46.9%.

Vibrational Spectra. The dialkyltellurium(IV) difluorides **1–5** show intense peaks corresponding to the TeF stretching

- (20) (a) Herberg, S.; Naumann, D. *Z. Anorg. Allg. Chem.* **1982**, *492*, 95. (b) Ruppert, I. *Chem. Ber.* **1979**, *112*, 3023.
- (21) Huheey, J. E.; Evans, R. S. *J. Inorg. Nucl. Chem.* **1970**, *32*, 383.
- (22) On one occasion a saturated solution of isopropyltellurium triazide (**14**) in methylene chloride exploded and resulted in pulverization of the glass vessel!

vibration²³ $\nu_{\text{TeF}} \sim 480 \text{ cm}^{-1}$ in their IR and Raman spectra (for assignments see Experimental Section).

The TeC stretching vibration ($\nu_{\text{TeC}} \sim 500 \text{ cm}^{-1}$)¹⁹ is assigned in the Raman spectra of **1–5** to intense peaks in the range of 561–495 cm⁻¹. The diazides **6–10** show the medium intense TeC stretching vibration in the 550–492 cm⁻¹ region of their Raman spectra. In contrast to **1–10**, where ν_{TeC} can be assigned, the TeC stretching vibration in the aryl derivatives $(\text{C}_6\text{H}_5)_2\text{Te}(\text{N}_3)_2$ and $(\text{C}_6\text{F}_5)_2\text{Te}(\text{N}_3)_2$ is lower in intensity and not characteristic, because other vibrations of the aromatic moiety overlap.¹² For the triazides, only **11**, **12**, and **14** show weakly intense TeC stretching vibrations in the IR and Raman spectra at 559–496 cm⁻¹.

The TeN stretching vibrations (ν_{TeN}) are detected around 350 cm⁻¹ as very intense peaks. In the case of $(\text{C}_6\text{H}_5)_2\text{Te}(\text{N}_3)_2$,¹² the vibration occurs at 330 cm⁻¹ and is the lowest TeN stretch, when compared with the diazides **6–10** at 355–346 cm⁻¹ and $(\text{C}_6\text{F}_5)_2\text{Te}(\text{N}_3)_2$ ¹² ($\nu_{\text{TeN}} = 356/347 \text{ cm}^{-1}$). These values are shifted to considerably lower wavenumbers when compared with the reported IR spectra of TeCl_3N_3 ($\nu_{\text{s,TeN}} = 412 \text{ cm}^{-1}$) and $\text{TeCl}_2(\text{N}_3)_2$ ($\nu_{\text{TeN}} = 413/400 \text{ cm}^{-1}$).⁷ Two very intense TeN stretching vibrations, accompanied by a shoulder, are found at 415–339 cm⁻¹ for the triazides **11–16**. All peaks of ν_{TeN} of the triazides are shifted to lower energies compared with the previously reported Raman data of $[\text{Te}(\text{N}_3)_3][\text{SbF}_6]$ ($\nu_{\text{s,TeN}} = 456 \text{ cm}^{-1}$).⁸

The antisymmetric azide stretching vibration $\nu_{\text{as,N}_3}$ is found for the diazides **6–10** as intense peaks in the IR spectra and medium intense peaks in the Raman spectra at 2092–2021 cm⁻¹. The $\nu_{\text{as,N}_3}$ vibration is slightly shifted to higher wavenumbers in the spectra of the triazides **11–16** and is observed as three to five peaks (IR strong, Raman medium intensity) at 2131–2028 cm⁻¹. The increased number of peaks reflects the presence of more than one azide species (axial and equatorial in triazides) bonded to tellurium in the solid state. The Raman spectrum of **11**, the simplest organotellurium(IV) triazide, is provided in the Supporting Information section. The observed frequencies, and also those of the diazide **6**, were calculated using density functional theory (DFT) methods and found to be in good agreement (see Quantum Chemical Computations).

NMR Spectra. The dialkyltellurium(IV) difluorides **2–5** show in the ¹⁹F NMR spectra extremely broad resonances (at 25 °C, 800–2200 Hz; see Experimental Section) for the TeF_2 fluorine atoms, which is due to the restricted rotation of the TeC bonds, a phenomenon observed and discussed in detail for diaryltellurium(IV) dihalides.²³ However, for methyl derivative **1**, a sharp resonance is observed at 25 °C, a septet, with ¹²⁵Te and ¹²³Te satellites visible. Similar to **1** but in contrast to **2**, free rotation of the TeC bonds in the ¹⁹F NMR spectra was reported for the perfluoroalkyl derivatives $(\text{CF}_3)_2\text{TeF}_2$ ²⁴ and $(\text{C}_2\text{F}_5)_2\text{TeF}_2$.²⁵ In general, the ¹⁹F

(23) Klapötke, T. M.; Krumm, B.; Mayer, P.; Polborn, K.; Ruscitti, O. P. *Inorg. Chem.* **2001**, *40*, 5169.

(24) (a) Herberg, S.; Naumann, D. *J. Fluorine Chem.* **1982**, *19*, 205. (b) Gomblér, W. Z. *Naturforsch., B* **1981**, *36b*, 535.

(25) Lau, C.; Passmore, J.; Richardson, E. K.; Whidden, T. K.; White, P. S. *Can. J. Chem.* **1985**, *63*, 2273.

NMR shifts of the alkyl derivatives in R_2TeF_2 **1–5** are fairly sensitive to R substituent and are thus found in a relatively wide range between $\delta = 125$ and 153 , the perfluoroalkyl substituted at $\delta = 125/117$ ($\text{R} = \text{CF}_3/\text{C}_2\text{F}_5$); bis(polyfluorophenyl)tellurium(IV) difluorides are shifted to high frequency and are in the region of $\delta \sim 100$.²³ The ¹²⁵Te NMR resonances of **1–5** are found at $\delta = 1380–1232$ and are shifted to high frequency as well relative to those of the bis(polyfluorophenyl)tellurium(IV) difluorides, which appear in the region of $\delta \sim 1080$.²³

The ¹²⁵Te resonances of the tellurium diazides **6–10** ($\delta = 1147–835$) are compared with the corresponding difluorides **1–5** shifted to lower frequency. This is due to the lower electronegativity of the azide group compared to fluorine, which leads to less deshielding of the tellurium nucleus. The ¹²⁵Te resonances of the tellurium triazides **11–16** are found at $\delta = 1405–1252$, which is, as expected, a significant high-frequency shift when compared with the resonances of the diazides. Here, the phenyl substituents in **15** and **16** cause a low-frequency shift relative to alkyl substituents in **11–14**.

A relatively sharp resonance (~ 50 Hz) is found at $\delta = 140$ for the symmetric β -nitrogen (connectivity $\text{Te}=\text{N}_\alpha-\text{N}_\beta=\text{N}_\gamma$) in the ¹⁴N NMR spectra of the tellurium di/triazides. The ¹⁴N resonance for the γ -nitrogen is detected from $\delta = 189$ to 250 and varies in its line width (70–2000 Hz). The α -nitrogen is visible at $\delta = 290$ to 325 ; for the triazides **12–15** the α -nitrogen resonance is too broad to be detected (line widths see Experimental Section). Unfortunately, the solubility of the di- and triazides is too low for natural abundance ¹⁵N NMR spectroscopy.

Description of the Crystal Structures. The molecular structures of the novel tellurium(IV) triazides (**12**, **13**, **14**, and **16**) were determined. All triazides, except **14**, are poorly soluble in chloroform and dichloromethane. Suitable crystals were obtained by cooling the filtered reaction mixtures. Crystal data and structure refinements are given in Table 1 and selected bond lengths and angles in Table 2. The molecular structures are shown in Figures 1–4.

The $\text{Te}-\text{C}_{\text{eq}}$ bond distance is 2.13 Å for **12**, **13**, and **16**; the $\text{Te}-\text{C}_{\text{eq}}$ bond length for **14** is slightly elongated, with 2.163(4) Å.

All the experimentally determined structures of tellurium(IV) triazides consist of two different azide substituents, one at the equatorial position and two at the axial positions. The difference is reflected in the $\text{Te}-\text{N}$ bond distances, which is ~ 2.05 Å for equatorial and ~ 2.22 Å for axial azides. The $\text{Te}-\text{N}$ bond distances in **12**, **13**, **14**, and **16** and in $(\text{C}_6\text{H}_5)_2\text{Te}(\text{N}_3)_2$ (2.253(3)/2.204(3) Å) and $(\text{C}_6\text{F}_5)_2\text{Te}(\text{N}_3)_2$ (2.208(2)/2.185(2) Å)¹² are significantly longer than those found in $\text{Te}(\text{N}_3)_3^+$ (1.994(7) Å).⁸ The $\text{Te}-\text{N}$ bond distance in $\text{Te}(\text{N}_3)_3^+$ is identical with the value of the covalent single bond distance $d(\text{TeN}_{\text{cov}}) = 1.99$ Å. Considerably longer $\text{Te}-\text{N}$ bond distances were found in the structures of $[(\text{C}_6\text{H}_5)_2\text{TeN}_3]_2\text{O}$ (2.397(8) Å)¹⁰ and $[(\text{C}_6\text{H}_5)_2\text{Te}(\text{NCS})]_2\text{O}$ (2.40(1) Å)²⁶ and

(26) Mancinelli, C. S.; Titus, D. D.; Ziolo, R. F. *J. Organomet. Chem.* **1977**, *140*, 113.

Table 1. Crystallographic Data for **12**, **13**, **14**, and **16**

	12	13	14	16
empirical formula	C ₂ H ₅ N ₉ Te	C ₃ H ₇ N ₉ Te	C ₃ H ₇ N ₉ Te	C ₉ H ₁₁ N ₉ Te
formula weight	282.72	296.75	296.75	372.84
temperature (°C)	-73(2)	-73(2)	-73(3)	-73(3)
color	colorless	colorless	colorless	yellow
crystal size (mm)	0.13 × 0.10 × 0.07	0.40 × 0.12 × 0.07	0.18 × 0.05 × 0.02	0.20 × 0.18 × 0.06
crystal system	monoclinic	monoclinic	monoclinic	monoclinic
space group	P2 ₁ /n	P2 ₁ /n	C2/c	P2 ₁ /c
<i>a</i> (Å)	8.4530(2)	8.7999(2)	20.058(2)	7.5503(6)
<i>b</i> (Å)	7.9094(2)	7.9674(2)	6.9620(3)	23.581(1)
<i>c</i> (Å)	12.6288(3)	13.2334(3)	15.030(1)	7.5094(6)
β (deg)	91.876(1)	94.626(1)	114.260(9)	91.295(9)
<i>V</i> (Å ³)	843.89(4)	924.80(4)	1913.5(2)	1336.6(2)
<i>Z</i>	4	4	8	4
ρ_{calcd} (g cm ⁻³)	2.225	2.131	2.060	1.853
μ (cm ⁻¹)	34.90	31.90	30.84	22.29
reflins collected	12252	13511	6478	8496
reflins unique	1485 ($R_{\text{int}} = 0.0758$)	2114 ($R_{\text{int}} = 0.0500$)	1854 ($R_{\text{int}} = 0.0465$)	2575 ($R_{\text{int}} = 0.0429$)
R1, wR2 ^a (2σ data)	0.0284, 0.0765	0.0244, 0.0621	0.0238, 0.0448	0.0228, 0.0536
R1, wR2 ^a (all data)	0.0395, 0.1026	0.0372, 0.0892	0.0389, 0.0469	0.0283, 0.0549
GOF <i>s</i> ^b on <i>F</i> ²	1.249	1.225	0.878	0.992

^a R1 = ($\sum ||F_o| - |F_c||$) / $\sum |F_o|$. wR2 = { $\sum [w(F_o^2 - F_c^2)^2] / \sum [w(F_o^2)^2]$ }^{1/2} with $w^{-1} = \sigma^2(F_o^2) + (xP)^2 + yP$. ^b *s* = { $\sum [w(F_o^2 - F_c^2)^2] / (N_o - N_p)$ }^{1/2}.

Table 2. Selected Bond Lengths (Å) and Angles (deg) for **12**, **13**, **14**, and **16**

	12	13	14	16
Te-C	2.128(6)	2.137(5)	2.163(4)	2.126(3)
Te-N _α (eq)	2.062(4)	2.066(3)	2.050(4)	2.047(2)
Te-N _α (ax)	2.251(4), 2.194(3)	2.244(3), 2.202(3)	2.182(3), 2.233(3)	2.180(2), 2.213(2)
N _α -N _β (eq)	1.231(6)	1.240(5)	1.226(5)	1.227(4)
N _β -N _γ (eq)	1.132(6)	1.125(5)	1.113(5)	1.132(4)
N _α -N _β (ax)	1.222(5), 1.203(5)	1.228(5), 1.215(4)	1.214(5), 1.203(5)	1.217(4), 1.192(3)
N _β -N _γ (ax)	1.139(6), 1.157(6)	1.129(5), 1.147(5)	1.140(5), 1.136(5)	1.134(4), 1.147(4)
C-Te-N(eq)	94.9(2)	95.2(2)	99.9(2)	104.7(1)
C-Te-N(ax)	87.6(2), 87.8(2)	88.5(2), 86.8(2)	84.3(2), 84.9(2)	89.1(1), 89.92(9)
N(eq)-Te-N(ax)	76.2(2), 85.2(2)	75.7(1), 86.6(1)	80.1(1), 86.5(2)	80.7(1), 88.1(1)
N(ax)-Te-N(ax)	160.4(1)	161.1(1)	161.1(1)	168.1(1)
Te-N(eq)-N(eq)	117.5(3)	116.9(2)	118.3(3)	116.5(2)
Te-N(ax)-N(ax)	113.1(3), 115.9(3)	113.5(2), 115.6(2)	117.3(3), 118.5(3)	116.1(2), 119.9(2)
N-N-N(eq)	173.6(4)	172.9(4)	173.4(5)	174.6(4)
N-N-N(ax)	175.3(5), 176.0(5)	176.7(4), 176.4(4)	174.6(4), 177.2(4)	177.4(3), 176.6(3)

merely Te···N interactions in [(C₆H₅)₃Te]NCS (3.099(7) Å)²⁷ and [(C₆H₅)₃Te]NCO (2.99(1) Å).²⁸ The latter two compounds are saltlike with considerable ionic character. In the diazides and triazides that have been investigated, the N₃ moiety acts as a pseudohalogen (Pauling electronegativities χ_P : F, 4.0; Cl, 3.0; Br, 2.8; N₃, 2.95(9)) and is covalently coordinated to tellurium.

The N_α-N_β and N_β-N_γ bond distances of all azide groups in **12**, **13**, **14**, and **16** are very similar. The N_α-N_β distance ranges from 1.192(3) Å in **16** to 1.240(5) Å in **13**, and the N_β-N_γ distance ranges from 1.113(5) Å in **14** to 1.157(6) Å in **12**. These N-N bond distances are similar to those found in Te(N₃)₃⁺ (average bond distances N_α-N_β 1.24(1) Å, N_β-N_γ 1.12(1) Å). The N_α-N_β distances of **12**, **13**, **14**, and **16** are significantly shorter than a typical N-N single bond (1.44 Å), while the other N_β-N_γ bond is slightly longer than the N≡N triple bond in N₂ (1.098 Å).⁹ The azide groups are slightly bent with NNN angles between 172.9(4)^o in **13** and 177.4(3)^o in **16**, as is the case in Te(N₃)₃⁺ (average N_α-N_β-N_γ 173.7(9)^o).⁸ The Te-N_α-N_β bond angle (range from 113.1(3)^o to 119.9(2)^o) is also quite similar to the corresponding angle in Te(N₃)₃⁺ (116.5(6)^o).⁸

(27) Lee, J.-S.; Titus, D. D.; Ziolo, R. F. *Inorg. Chem.* **1977**, *16*, 2487.

(28) Lee, J.-S.; Titus, D. D.; Ziolo, R. F. *J. Organomet. Chem.* **1976**, *120*, 381.

The N-Te-N (N_{eq}-Te-N_{ax}, N_{eq}-Te-N_{ax}, N_{ax}-Te-N_{ax}) angles in **12** (76.2(2)^o, 85.2(2)^o, and 160.4(1)^o) and **13** (75.7(1)^o, 86.6(1)^o, and 161.1(1)^o) are quite similar, due to a similar sterical arrangement of the ethyl and *n*-propyl groups. The N-Te-N angles in **14** are 80.1(1)^o, 86.5(2)^o, and 161.1(1)^o. Comparing **12**, **13**, and **14** with **16** (N-Te-N angles of 80.7(1)^o, 88.1(1)^o, and 168.1(1)^o), a distinct difference in the angle of the two axial azide groups with tellurium (N_{ax}-Te-N_{ax}) is obvious, corresponding to the larger steric demand of the mesityl group.

A steric arrangement similar to that found in (C₆H₅)₂Te-(N₃)₂ and (C₆F₅)₂Te(N₃)₂¹² was found for **16**. Both axial azides are bent toward the phenyl substituents and away from the tellurium electron pair in (C₆H₅)₂Te(N₃)₂, and in (C₆F₅)₂Te(N₃)₂ the two azide groups are bent away from the fluorinated phenyl rings and toward the tellurium electron pair. This effect is likely of steric origin and electrostatic repulsions between free electron pairs of fluorine and nitrogen. Both axial azide groups in **16** are bent toward the mesityl ring and away from the tellurium(IV) electron pair (located in the equatorial plane), as was similarly found for (C₆H₅)₂Te(N₃)₂, finding an energetically favorable conformation. Furthermore, this indicates that in (C₆F₅)₂Te(N₃)₂ the fluorine atoms of the perfluorinated phenyl ring are respon-

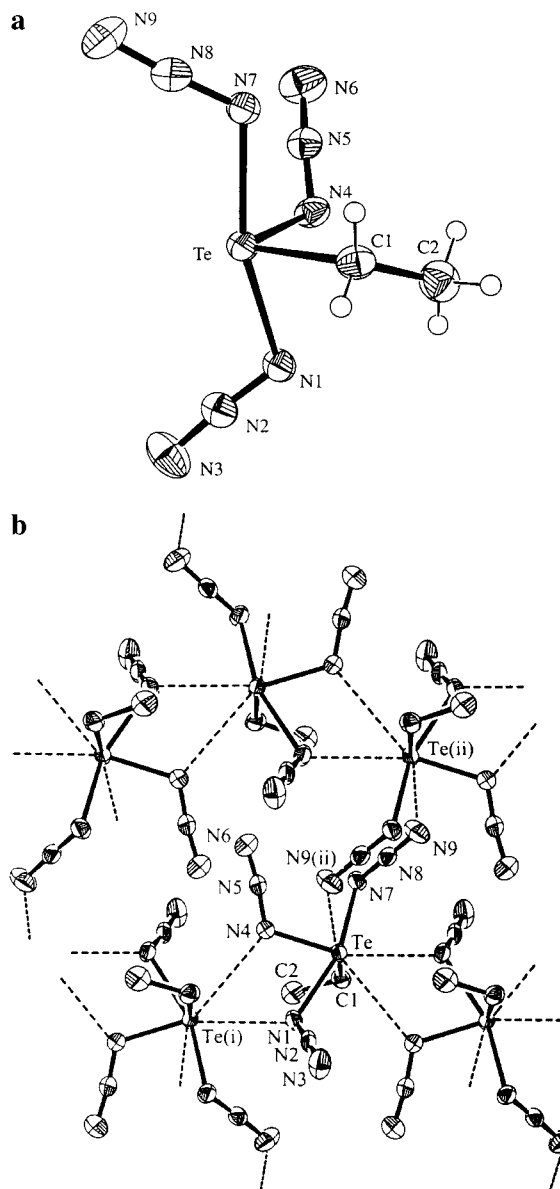


Figure 1. (a) Molecular structure of $\text{C}_2\text{H}_5\text{Te}(\text{N}_3)_3$ (**12**) with thermal ellipsoids at the 50% probability level. (b) Polymer structure of **12** (only selected atoms are labeled for clarity) showing $\text{Te}\cdots\text{N}$ interactions. Selected interactions, lengths (\AA) and angles (deg): $\text{Te}(i)\cdots\text{N}(1)$ 2.789(4), $\text{Te}(i)\cdots\text{N}(4)$ 3.187(4), $\text{Te}\cdots\text{N}(9(ii))$ 3.129(5); $\text{Te}(i)\cdots\text{N}(1)-\text{Te}$ 119.7(1), $\text{Te}(i)\cdots\text{N}(4)-\text{Te}$ 110.8(2), $\text{N}(1)-\text{Te}(i)\cdots\text{N}(4)$ 52.5(1) with $i = -x + 1 \frac{1}{2}, y - \frac{1}{2}, -z + \frac{1}{2}$ and $ii = -x + 2, -y + 1, -z + 1$.

sible for the more unusual steric arrangement of the azide groups.

The tellurium triazides **12** (Figure 1a), **13** (Figure 2a), **14** (Figure 3a), and **16** (Figure 4a) show in the first approximation a Ψ -trigonal-bipyramidal geometry around tellurium. In addition, all compounds that have been studied exhibit unique intermolecular tellurium–nitrogen interactions in the range of 2.79–3.29 \AA , which are shorter than the sum of their van der Waals radii (vdWr TeN 3.61 \AA).²⁹ These $\text{Te}\cdots\text{N}$ interactions result in extended coordination spheres around tellurium (Figures 1b, 2b (Supporting Information section), 3b, and 4b). Intermolecular interactions of the

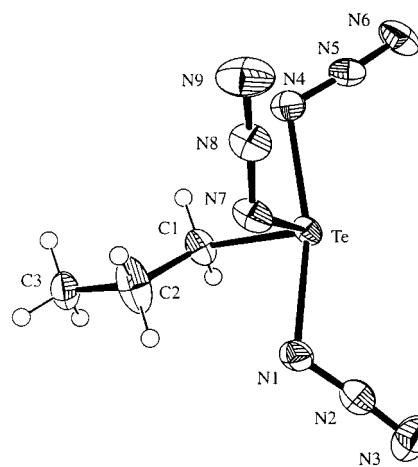


Figure 2. (a) Molecular structure of $n\text{-C}_3\text{H}_7\text{Te}(\text{N}_3)_3$ (**13**) with thermal ellipsoids at the 50% probability level. Figure 2b (polymer structure of **13**) not shown, identical to Figure 1b (see Supporting Information). Selected interactions, lengths (\AA) and angles (deg): $\text{Te}\cdots\text{N}(6(i))$ 3.226(4), $\text{Te}(iii)\cdots\text{N}(1)$ 2.831(3), $\text{Te}(iii)\cdots\text{N}(7)$ 3.244(3), $\text{Te}(iii)\cdots\text{N}(1)-\text{Te}$ 120.2(1), $\text{Te}(iii)\cdots\text{N}(7)-\text{Te}$ 110.3(1), $\text{N}(1)-\text{Te}(iii)\cdots\text{N}(7)$ 51.12(8) with $i = -x + 1, -y + 1, -z + 2$ and $iii = -x + \frac{1}{2}, y - \frac{1}{2}, -z + 1 \frac{1}{2}$.

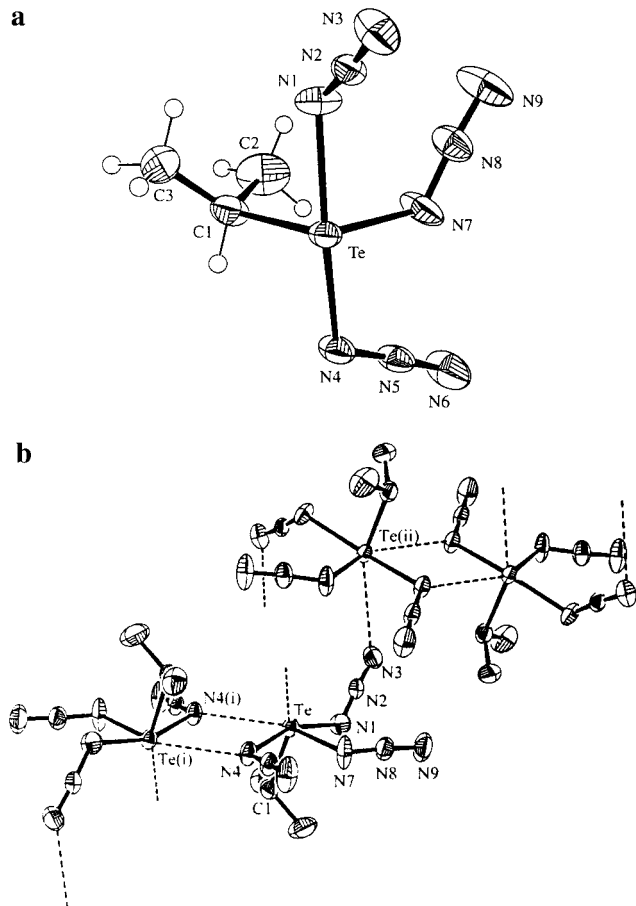


Figure 3. (a) Molecular structure of $i\text{-C}_3\text{H}_7\text{Te}(\text{N}_3)_3$ (**14**) with thermal ellipsoids at the 50% probability level. (b) Polymer structure of **14** (only selected atoms are labeled for clarity) showing $\text{Te}\cdots\text{N}$ interactions. Selected interactions, lengths (\AA) and angles (deg): $\text{Te}(i)\cdots\text{N}(4)$ 2.852(3), $\text{Te}(ii)\cdots\text{N}(3)$ 3.290(4); $\text{N}(4)-\text{Te}\cdots\text{N}(4(i))$ 66.5(1), $\text{N}(1)-\text{Te}\cdots\text{N}(4(i))$ 125.8(1) with $i = -x + 1 \frac{1}{2}, -y + \frac{1}{2}, -z + 1$ and $ii = -x + 1 \frac{1}{2}, y - \frac{1}{2}, -z + 1 \frac{1}{2}$.

α -nitrogen atom of two azide groups (one axial and one equatorial) and the γ -nitrogen atom of an azide group of a second molecule with a tellurium atom of a third molecule

(29) Bondi, A. *J. Phys. Chem.* **1964**, *68*, 441.

Table 3. Computational Results for $(CH_3)_2Te(N_3)_2$ (**6**) and $CH_3Te(N_3)_3$ (**11**)

	MPW1PW91/3-21G(d)	MPW1PW91/ECP46MWB+D95V	MPW1PW91/ECP46MWB+[5s5p1d]/(3s3p1d) (Te) and 6/311G(d,p) (H, C, N)
$-E/\text{au}$	6992.147 922	$(CH_3)_2Te(N_3)_2$ 416.047 881	416.262 632
ZPE/kcal mol ⁻¹	62.4	63.0	62.9
NIMAG	0	0	0
$d(\text{Te}-\text{N}_{\text{ax}})/\text{\AA}$	2.180	2.217	2.221
$d(\text{Te}-\text{C}_{\text{eq}})/\text{\AA}$	2.140	2.122	2.118
$\angle(\text{N}-\text{Te}-\text{N})/\text{deg}$	163.4	163.9	165.6
$\angle(\text{C}-\text{Te}-\text{C})/\text{deg}$	96.9	96.7	97.0
$-E/\text{au}$	7115.662 372	$CH_3Te(N_3)_3$ 540.227 366	540.521 499
ZPE/kcal mol ⁻¹	46.2	46.6	47.7
NIMAG	0	0	0
$d(\text{Te}-\text{N}_{\text{ax},\text{av}})/\text{\AA}$	2.146	2.164	2.176
$d(\text{Te}-\text{N}_{\text{eq}})/\text{\AA}$	2.090	2.111	2.086
$d(\text{Te}-\text{C}_{\text{eq}})/\text{\AA}$	2.131	2.115	2.110
$\angle(\text{N}_{\text{ax}}-\text{Te}-\text{N}_{\text{ax}})/\text{deg}$	161.9	162.7	163.8
$\angle(\text{C}-\text{Te}-\text{N}_{\text{eq}})/\text{deg}$	99.1	99.3	98.8
$\angle(\text{N}_{\text{ax}}-\text{Te}-\text{C}_{\text{eq}})/\text{deg}$	82.9	83.2	84.4

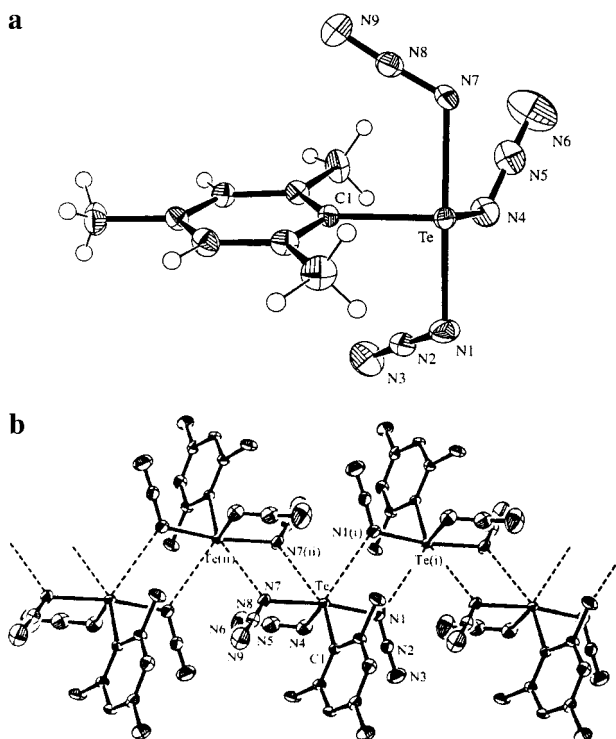


Figure 4. (a) Molecular structure of 2,4,6-(CH₃)₃C₆H₂Te(N₃)₃ (**16**) with thermal ellipsoids at the 50% probability level. (b) Polymer structure of **16** (only selected atoms are labeled for clarity) showing Te...N interactions. Selected interactions, lengths (Å) and angles (deg): Te(i)...N(1) 3.234(3), Te(ii)...N(7) 3.031(2); Te(ii)...N(7)-Te 115.11(4), Te-N(1)...Te(i) 115.51(4), N(7)-Te...N(7(ii)) 64.89(9), N(7)-Te...N(1(i)) 123.60(8) with $i = -x + 1, -y, -z$ and $ii = -x + 1, -y, -z + 1$.

in **12** (2.789(4), 3.187(4), and 3.129(5) Å) and **13** (2.831(3), 3.244(3), and 3.226(3) Å) form polymeric structures, resulting in octacoordination of each tellurium atom. The structure of the isopropyl derivative **14** differs slightly from those of the *n*-alkyl derivatives. It consists of infinite chains of Te₂N₂ units (2.233(3), 2.852(3) Å), which are linked by a Te...N_γ interaction (3.290(4) Å) plus another weaker interaction (3.339(4) Å, not shown). The isopropyl groups are arranged in a trans fashion. Two α-nitrogen and two tellurium atoms

form a planar four-membered Te₂N₂ ring (the torsion angle of Te-N[•]...Te-N is 0°). Other four-membered tellurium–nitrogen heterocycles with shorter, more single bond character of Te–N have been reported.³⁰

A different motif is found for **16**, where two axial azide groups exhibit intramolecular interactions (3.031(2), 3.234(3) Å). Each tellurium atom in the polymeric chain of **16** is connected to two α-nitrogens belonging to two different molecules, leading to heptacoordination around Te. This effect is also observed for (C₆H₅)₂Te(N₃)₂ and (C₆F₅)₂Te(N₃)₂,¹² which seems to be a characteristic feature of aryl-substituted tellurium(IV) azides.

Quantum Chemical Computations. For both (CH₃)₂Te(N₃)₂ (**6**) and CH₃Te(N₃)₃ (**11**) the energies, zero point energies, and IR as well as Raman intensities were computed at the electron correlated hybrid DFT MPW1PW91 level of theory using an all-electron basis set as well as a core potential with two different valence basis sets. The results are summarized in Tables 3 and 4. The fully optimized molecular structures of **6** and **11** are shown in Figure 5. The computed vibrational frequencies are in very good agreement with the experimental IR and Raman data at all levels of theory applied. This gives credence also to the computed structural parameters of the methyl compounds, for which at present there are no experimental data available. The calculated bond lengths and angles for CH₃Te(N₃)₃ (**11**) also agree well with those of the crystal structure of C₂H₅Te(N₃)₃ (**12**); therefore, calculations were omitted for **12**.

Conclusion

The synthesis and spectroscopic studies of dialkyltellurium(IV) difluorides, dialkyltellurium(IV) diazides, and the first covalent alkyl/aryltellurium(IV) triazides were described. Single-crystal X-ray diffraction studies show polymeric networks with tellurium–nitrogen interactions leading to

(30) (a) Chivers, T.; Gao, X.; Sandblom, N.; Schatte, G. *Phosphorus, Sulfur, Silicon Relat. Elem.* **1998**, 136–138, 11 and references therein. (b) Lau, C.; Krautschied, H.; Neumüller, B.; Dehnicke K. *Z. Anorg. Allg. Chem.* **1997**, 623, 1375.

Table 4. Selected Computed Vibrational Data for $(\text{CH}_3)_2\text{Te}(\text{N}_3)_2$ (**6**) and $\text{CH}_3\text{Te}(\text{N}_3)_3$ (**11**)^a

	MPW1PW91/3-21G(d)	MPW1PW91/ECP46MWB+D95V	MPW1PW91/ECP46MWB+[5s5p1d]/(3s3p1d) (Te) and 6/311G(d,p) (H, C, N)	exptl data IR/ Raman (rel int)
$(\text{CH}_3)_2\text{Te}(\text{N}_3)_2$				
$\nu_{\text{as}}(\text{NNN}_{\text{ax},\text{ip}})$	2056 (371/73)	2111 (477/228)	2266 (729/171)	-/2051 (21)
$\nu_{\text{as}}(\text{NNN}_{\text{ax},\text{oop}})$	2033 (1354/38)	2088 (1794/99)	2239 (1703/100)	2028 (s)/2046 (19)
$\nu_{\text{sym}}(\text{NNN}_{\text{ip}})$	1235 (62/13)	1312 (60/16)	1375 (101/14)	1318 (m)/1323 (5)
$\nu_{\text{sym}}(\text{NNN}_{\text{oop}})$	1227 (283/7)	1305 (291/7)	1366 (297/6)	1260 (m)/1270 (7)
$\nu(\text{TeC}_{\text{oop}})$			560 (0/23)	-/550 (24)
$\nu(\text{TeC}_{\text{ip}})$			554 (0/44)	545 (w)/540 (43)
$\nu(\text{TeN}_{\text{oop}})$	397 (220/2)	329 (238/2)	341 (280/1)	-/-
$\nu(\text{TeN}_{\text{ip}})$	381 (0/56)	322 (0/170)	353 (0/96)	-/346 (100)
$\text{CH}_3\text{Te}(\text{N}_3)_3$				
$\nu_{\text{as}}(\text{NNN}_{\text{ax},\text{ip}})$	2071 (373/108)	2130 (418/256)	2281 (532/226)	2097(m)/2101(18)
$\nu_{\text{as}}(\text{NNN}_{\text{ax}})$	2056 (602/40)	2113 (1216/127)	2268 (801/99)	2062(vs)/2075(6)
$\nu_{\text{as}}(\text{NNN}_{\text{ax},\text{oop}})$	2036 (918/44)	2095 (706/82)	2247 (1269/99)	2031(vs)/2034(18)
$\nu_{\text{sym}}(\text{NNN}_{\text{ax},\text{ip}})$	1217 (80/9)	1319 (123/10)	1364 (101/10)	1316 (m)/1320 (5)
$\nu_{\text{sym}}(\text{NNN}_{\text{ax},\text{oop}})$	1206 (336/5)	1302 (296/7)	1353 (362/4)	1260 (m)/1263 (5)
$\nu_{\text{sym}}(\text{NNN}_{\text{eq}})$	1157 (139/1)	1247 (140/5)	1315 (156/1)	1229 (m)/1233 (5)
$\nu(\text{TeC})$			558 (1/35)	-/559 (33)
$\nu(\text{TeN}_{\text{ip}})$	426 (16/62)	366 (22/154)	399 (11/98)	-/402 (100)
$\nu(\text{TeN}_{\text{oop}})$	418 (190/6)	352 (194/12)	370 (154/13)	-/380 (35)
$\nu(\text{TeN}_{\text{oop}})$	389 (25/13)	323 (29/23)	351 (124/9)	-/371 (46)

^a Wavenumbers in cm^{-1} , IR intensities in km mol^{-1} , Raman scattering activities in $\text{\AA}^4 \text{ amu}^{-1}$, ip = in phase, oop = out of phase.

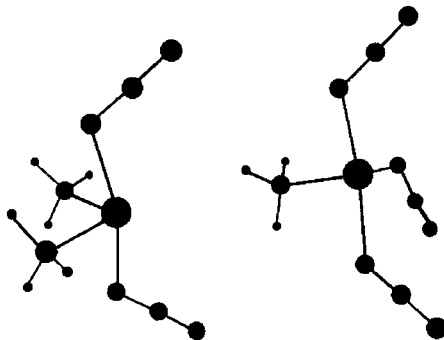


Figure 5. Calculated structures of, left, $(\text{CH}_3)_2\text{Te}(\text{N}_3)_2$ (**6**) and, right, $\text{CH}_3\text{Te}(\text{N}_3)_3$ (**11**).

hepta- or octacoordination of the tellurium atom. Quantum chemical computations of the methyl derivatives using a hybrid DFT method are in good agreement with the results obtained by vibrational spectroscopy.

Experimental Section

Caution! Covalent tellurium azides are potentially explosive; small-scale syntheses are recommended. The azides discussed here should be handled with extreme care and safety precautions; i.e., fully protective clothing (face shield, gloves, coat) should be worn at all times and appropriate shielding should be used.

Materials. Dichloromethane was distilled and stored under dry nitrogen prior to use. Xenon difluoride (FluoroChem) and trimethylsilyl azide (Aldrich) were used as received. Dialkyl tellurides and dialkyl/aryl ditellurides were prepared by literature methods.^{16–19} Dimethyl telluride was prepared by a procedure similar to that outlined for dimethyl ditelluride.^{16b}

General Considerations. All reactions were carried out with standard Schlenk techniques under dry nitrogen gas. All compounds were dried and purified for several hours under high vacuum. Infrared spectra were recorded as neat liquids or Nujol mulls on a Nicolet 520 FT-IR spectrometer between KBr plates; Raman spectra were recorded on a Perkin-Elmer Spectrum 2000 NIR FT-Raman spectrometer as neat solids or liquids (1064 nm, Nd:YAG laser, glass capillary). All NMR spectra were obtained on a JEOL 400

Eclipse instrument using CDCl_3 as solvent except where otherwise indicated. The chemical shifts were referenced with respect to $(\text{CH}_3)_4\text{Si}$ (^1H , ^{13}C), CH_3NO_2 (^{14}N), CFCl_3 (^{19}F), and $(\text{CH}_3)_2\text{Te}$ (^{125}Te). Due to the temperature dependence of the ^{125}Te shifts, all samples were recorded at 25 °C. Mass spectra were recorded on a Finnigan MAT 95Q spectrometer using electron impact (EI) techniques. Multiisotope-containing fragments refer to the isotope with the highest abundance. Elemental analyses C, H, N were performed by the analytical service of the Department of Chemistry, LMU. Elemental analyses were not performed for the tellurium triazides because of the potential danger of explosion. Melting points were determined on a Büchi B540 instrument.

X-ray Crystallography. For single-crystal structure determination, a Nonius Kappa CCD (**12**, **13**) or a Stoe IPDS area detector (**14**, **16**) was employed for data collection using Mo $\text{K}\alpha$ radiation ($\lambda = 0.71073 \text{ \AA}$). For **12**, **13**, **14**, and **16**, the structures were solved by direct methods (SIR97) and refined using SHELXL-97 (Table 1). All non-hydrogen atoms were refined anisotropically. A numerical absorption correction was performed.

Programs and Methods. All calculations were performed with the program package Gaussian 98.³¹ The structures were fully optimized at MPW1PW91 level of theory using a ECP-46-MWB and a [5s5p1d]/(3s3p1d) valence basis set for Te and a 6/311G-(d,p) basis set for H, C, and N without symmetry constraints. The vibrational frequencies were computed using the optimized structures. The vibrational spectra and molecular structure diagrams were generated from the Gaussian output files of the fully optimized structure using the program package GaussView 2.1.³² All struc-

- (31) Frisch, M. J.; Trucks, G. W.; Schlegel, H. B.; Scuseria, G. E.; Robb, M. A.; Cheeseman, J. R.; Zakrzewski, V. G.; Montgomery, Jr., J. A.; Stratmann, R. E.; Burant, J. C.; Dapprich, S.; Millam, J. M.; Daniels, A. D.; Kudin, K. N.; Strain, M. C.; Farkas, O.; Tomasi, J.; Barone, V.; Cossi, M.; Cammi, R.; Mennucci, B.; Pomelli, C.; Adamo, C.; Clifford, S.; Ochterski, J.; Petersson, G. A.; Ayala, P. Y.; Cui, Q.; Morokuma, K.; Malick, D. K.; Rabuck, A. D.; Raghavachari, K.; Foresman, J. B.; Cioslowski, J.; Ortiz, J. V.; Stefanov, B. B.; Liu, G.; Liashenko, A.; Piskorski, P.; Komaromi, I.; Gomperts, R.; Martin, R. L.; Fox, D. J.; Keith, T.; Al-Laham, M. A.; Peng, C. Y.; Nanayakkara, A.; Gonzalez, C.; Challacombe, M.; Gill, P. M. W.; Johnson, B.; Chen, W.; Wong, M. W.; Andres, J. L.; Gonzalez, C.; Head-Gordon, M.; Replogle, E. S.; Pople, J. A. *Gaussian* 98, Revision A.3; Gaussian, Inc.: Pittsburgh, PA, 1998.
- (32) GaussView 2.1; Gaussian, Inc.: Pittsburgh, PA, 2000.

tures, energies, zero point energies (ZPE), and vibrational data were calculated at the electron-correlated MPW1PW91^{33–37} hybrid DFT level of theory using both all-electron calculations and applying a quasirelativistic core potential for Te.^{38,39}

General Procedure for the Preparation of R₂TeF₂ (R = CH₃, C₂H₅, n-C₃H₇, i-C₃H₇, c-C₆H₁₁). Into a solution of 3.4 mmol of R₂Te in 15 mL of CH₂Cl₂ was added 3.5 mmol of XeF₂ at –50 °C. After stirring for 30 min at –50 °C and a further 30 min at 25 °C, the volatile materials were removed in vacuo, leaving pure compounds R₂TeF₂.

Properties and Spectral Data for (CH₃)₂TeF₂ (1). Colorless solid, yield 91%, mp 79–81 °C; IR 3020 s, 2927 s, 1643 m, 1465 m, 1402 m, 1233 m, 873 m, 566 m cm^{–1}; Raman 3025 (14), 2933 (46), 1409 (3), 1244 (4), 1233 (4), 561 (100, ν_{TeC}), 479 (27, ν_{TeF}), 454 (28), 245 (22), 178 (7), 111 (4) cm^{–1}; ¹H NMR δ 2.57 (t, ³J_{H–F} = 7.3 Hz); ¹⁹F NMR δ –124.9 (sept, ¹J_{F–¹²⁵Te} = 870.9 Hz, ¹J_{F–¹²³Te} = 721.8 Hz); ¹³C NMR δ 22.8 (t, ²J_{C–F} = 10.4 Hz, ¹J_{C–Te} = 214.1 Hz); ¹²⁵Te NMR δ 1232 (tsept, ¹J_{Te–F} = 871.1 Hz, ²J_{Te–H} = 22.2 Hz); MS (EI) [m/e (¹³⁰Te) (intensity, species)] 183 (18, M⁺ – CH₃), 179 (100, M⁺ – F), 168 (2, TeF₂⁺), 160 (5, M⁺ – 2F), 149 (4, TeF⁺), 145 (4, CH₃Te⁺), 130 (3, Te⁺). Anal. Calcd for C₂H₆F₂Te (195.67): C, 12.3; H, 3.1. Found: C, 12.4; H, 3.2.

Properties and Spectral Data for (C₂H₅)₂TeF₂ (2). Colorless liquid, yield 88%; IR 2965 s, 2935 s, 2877 s, 2862 m, 1723 m, 1599 w, 1580 w, 1455 s, 1411 m, 1382 m, 1287 m, 1213 s, 1122 m, 1072 m, 1040 m, 967 m, 884 m, 766 m, 740 s, 637 w, 611 m, 575 s, 481 vs (ν_{TeF}), 450 vs cm^{–1}; Raman 2975 (44), 2937 (100), 2878 (32), 2740 (7), 1460 (13), 1227 (18), 1209 (15), 1037 (7), 521 (98, ν_{TeC}), 481 (36, ν_{TeF}), 312 (22), 301 (10), 289 (9), 193 (15) cm^{–1}; ¹H NMR δ 2.85 (CH₂, m, 4H), 1.47 (CH₃, m, 6H); ¹⁹F NMR (Δν_{1/2} [Hz]) δ –136 (vbr, 1200); ¹³C NMR δ 33.7 (CH₂, ¹J_{C–Te} = 207.1 Hz), 8.7 (CH₃, ²J_{C–Te} = 21.3 Hz); ¹²⁵Te{¹H} NMR δ 1316; MS (EI) [m/e (¹³⁰Te) (intensity, species)] 207 (16, M⁺ – F), 187 (12, M⁺ – 2F – H), 159 (21, C₂H₅Te⁺), 130 (19, Te⁺), 29 (100, C₂H₅⁺), 15 (8, CH₃⁺). Anal. Calcd for C₄H₁₀F₂Te (223.72): C, 21.5; H, 4.5. Found: C, 20.0; H, 4.3.

Properties and Spectral Data for (n-C₃H₇)₂TeF₂ (3). Colorless liquid, yield 91%; IR 2965 vs, 2933 s, 2873 s, 1835 w, 1725 m, 1460 vs, 1378 w, 1339 w, 1279 m, 1228 s, 1190 m, 1123 vw, 1083 m, 1032 w, 963 w, 899 w, 834 w, 740 m, 716 m, 641 w, 630 w, 575 m, 488 m (ν_{TeF}), 477 s, 451 vs, 405 s cm^{–1}; Raman 3326 (3), 3232 (4), 2935 (100), 2874 (50), 2738 (5), 1453 (29), 1407 (13), 1336 (14), 1285 (10), 1199 (25), 1078 (9), 1026 (25), 882 (9), 801 (6), 761 (6), 615 (61), 539 (56, ν_{TeC}), 488 (52, ν_{TeF}), 400 (25), 296 (50) cm^{–1}; ¹H NMR δ 2.97 (CH₂, t, ³J_{H–H} = 7.4 Hz, 4H), 1.98 (CH₂, m, 4H), 1.10 (CH₃, t, 6H); ¹⁹F NMR (Δν_{1/2} [Hz]) δ –127 (vbr, 1350); ¹³C NMR δ 43.5 (CH₂Te, ¹J_{C–Te} = 206.6 Hz), 18.0 (CH₂), 15.8 (CH₃); ¹²⁵Te{¹H} NMR δ 1291; MS (EI) [m/e (¹³⁰Te) (intensity, species)] 235 (5, M⁺ – F), 216 (M⁺ – 2F), 173 (25, C₃H₇Te⁺), 130 (5, Te⁺), 43 (100, C₃H₇⁺). Anal. Calcd for C₆H₁₄F₂Te (251.77): C, 28.6; H, 5.6. Found: C, 27.3; H, 5.4.

Properties and Spectral Data for (i-C₃H₇)₂TeF₂ (4). Colorless liquid, yield 93%; IR 2965 vs, 2926 vs, 2870 vs, 2767 m, 2729 m,

- (33) Adamo, C.; Barone V. *Chem. Phys. Lett.* **1997**, 274, 242.
- (34) Burke, K.; Perdew, J. P.; Wang, Y. In *Electron Density Functional Theory: Recent Progress and New Directions*; Dobson, J. F., Vignale, G., Das, M. P., Eds.; Plenum: New York, 1998.
- (35) Perdew, J. P.; Chevary, J. A.; Vosko, S. H.; Jackson, K. A.; Pederson, M. R.; Singh, D. J.; Fiolhais, C. *Phys. Rev. B* **1992**, 46, 6671.
- (36) Perdew, J. P.; Chevary, J. A.; Vosko, S. H.; Jackson, K. A.; Pederson, M. R.; Singh, D. J.; Fiolhais, C. *Phys. Rev. B* **1993**, 48, 4978.
- (37) Perdew, J. P.; Burke, K.; Wang, Y. *Phys. Rev. B* **1996**, 54, 16533.
- (38) Igel-Mann, G.; Stoll, H.; Preuss, H. *Mol. Phys.* **1988**, 65, 1321.
- (39) Bergner, A.; Dolg, M.; Kuechle, W.; Stoll, H.; Preuss, H. *Mol. Phys.* **1993**, 80, 1431.

1615 w, 1574 w, 1466 s, 1387 s, 1371 s, 1288 w, 1210 vs, 1158 vs, 1098 m, 1021 m, 955 m, 931 m, 875 m, 769 s, 708 s, 611 m, 484 s (ν_{TeF}), 451 vs, 419 vs cm^{–1}; Raman 2967 (47), 2931 (71), 2871 (36), 1459 (33), 1444 (30), 1390 (21), 1218 (41), 1160 (26), 875 (22), 617 (6), 515 (100, ν_{TeC}), 485 (55, ν_{TeF}), 419 (26), 362 (15), 266 (66), 178 (31), 117 (20) cm^{–1}; ¹H NMR δ 2.95 (CH, sept, ³J_{H–H} = 7.2 Hz, 2H), 1.35 (CH₃, d, 12H); ¹⁹F NMR (Δν_{1/2} [Hz]) δ –151 (vbr, 800); ¹³C NMR δ 45.0 (CH, ¹J_{C–Te} = 201.8 Hz), 18.6 (CH₃, ²J_{C–Te} = 33.4 Hz); ¹²⁵Te{¹H} NMR δ 1380 (br); MS (EI) [m/e (¹³⁰Te) (intensity, species)] 235 (5, M⁺ – F), 216 (15, M⁺ – 2F), 173 (25, C₃H₇Te⁺), 130 (5, Te⁺), 43 (100, C₃H₇⁺). Anal. Calcd for C₆H₁₄F₂Te (251.77): C, 28.6; H, 5.6. Found: C, 27.3; H, 5.6.

Properties and Spectral Data for (c-C₆H₁₁)₂TeF₂ (5). Colorless liquid, yield 75%; IR 2929 vs, 2852 vs, 1448 vs, 1333 s, 1299 m, 1257 s, 1228 w, 1177 s, 1047 w, 1026 m, 992 s, 916 m, 888 s, 865 w, 845 m, 807 m, 789 m, 738 m, 670 m, 642 w, 613 w, 481 s (ν_{TeF}), 454 vs cm^{–1}; Raman 3010 (16), 2940 (100), 2852 (82), 1444 (46), 1335 (22), 1304 (20), 1258 (35), 1180 (33), 1112 (17), 1025 (38), 993 (30), 846 (36), 810 (32), 674 (69), 495 (43, ν_{TeC}), 483 (65, ν_{TeF}), 432 (26), 246 (42), 204 (77) cm^{–1}; ¹H NMR δ 3.14 (CH, m, 2H), 2.14–1.25 (CH₂, 20H); ¹⁹F NMR (Δν_{1/2} [Hz]) δ –153 (vbr, 2200); ¹³C NMR δ 54.7 (CH, ¹J_{C–Te} = 210.2 Hz), 29.0 (C₂, ²J_{C–Te} = 25.8 Hz), 27.4 (C₃, ³J_{C–Te} = 23.1 Hz), 25.5 (C₄); ¹²⁵Te{¹H} NMR δ 1355; MS (EI) [m/e (¹³⁰Te) (intensity, species)] 426 (5, M⁺ – 2F + Te), 343 (5, C₆H₁₁Te₂⁺), 296 (23, M⁺ – 2F), 213 (16, C₆H₁₁Te⁺), 83 (100, C₆H₁₁⁺). Anal. Calcd for C₁₂H₂₂F₂Te (331.90): C, 43.4; H, 6.8. Found: C, 41.9; H, 6.8.

General Procedure for the Preparation of R₂Te(N₃)₂ (R = CH₃, C₂H₅, n-C₃H₇, i-C₃H₇, c-C₆H₁₁). Into a solution of 2.9 mmol of R₂TeF₂ in 15 mL of CH₂Cl₂ was added 6.1 mmol of Me₃SiN₃ at 0 °C. After stirring for 2 1/2 h at 0 °C and a further 30 min at 25 °C, the volatile materials were removed in vacuo, leaving pure compounds.

Properties and Spectral Data for (CH₃)₂Te(N₃)₂ (6). Colorless solid, yield 85%, mp 45–47 °C; IR 2028 vs (ν_{as,N₃}), 1403 w, 1318 m, 1260 m, 1093 m, 1023 m, 871 m, 800 m, 680 m, 649 m, 545 w (ν_{TeC}) cm^{–1}; Raman 2932 (18), 2051 (21)/2046 (19, ν_{as,N₃}), 1323 (5), 1270 (7), 652 (12), 550 (24)/540 (43, ν_{TeC}), 346 (100, ν_{TeN}), 230 (13), 179 (22), 138 (25) cm^{–1}; ¹H NMR δ 2.64 (²J_{H–Te} = 21.1 Hz); ¹³C NMR δ 17.4 (¹J_{C–Te} = 162.2 Hz); ¹²⁵Te NMR 835 (sept); ¹⁴N NMR (Δν_{1/2} [Hz]) δ –137 (30, N_β), –202 (70, N_γ), –294 (450, N_α); MS (EI) [m/e (¹³⁰Te) (intensity, species)] 202 (58, M⁺ – N₃), 187 (3, CH₃TeN₃⁺), 172 (2, TeN₃⁺), 160 (92, M⁺ – 2N₃), 145 (59, CH₃Te⁺), 130 (18, Te⁺), 57 (5, CH₃N₃⁺), 43 (100, HN₃⁺). Anal. Calcd for C₂H₆N₆Te (241.71): C, 9.9; H, 2.5; N, 34.8. Found: C, 10.8; H, 2.6; N, 32.6.

Properties and Spectral Data for (C₂H₅)₂Te(N₃)₂ (7). Colorless liquid, yield 96%; IR 2972 m, 2930 m, 2871 m, 2649 w, 2581 m, 2062 s/2026 vs (ν_{as,N₃}), 1449 m, 1408 m, 1377 m, 1314 m, 1258 m, 1227 m, 1045 w, 1027 w, 994 w, 963 m, 737 m, 648 m, 611 m, 524 w, 481 m cm^{–1}; Raman 2973 (7), 2934 (17), 2873 (4), 2092 (3)/2059 (9)/2024 (6, ν_{as,N₃}), 1452 (3), 1409 (2), 1380 (2), 1319 (6), 1267 (3), 1219 (5), 1049 (2), 648 (7), 520 (22)/503 (27, ν_{TeC}), 411 (10), 350 (100, ν_{TeN}), 306 (18), 187 (23 (23), 113 (25) cm^{–1}; ¹H NMR δ 3.05 (CH₂, q, ³J_{H–H} = 7.7 Hz, 4H), 1.67 (CH₃, t, 6H); ¹³C NMR δ 31.2 (CH₂, ¹J_{C–Te} = 154.1 Hz), 10.1 (CH₃, ²J_{C–Te} = 20.4 Hz); ¹²⁵Te{¹H} NMR δ 997 (br); ¹⁴N NMR (Δν_{1/2} [Hz]) δ –137 (50, N_β), –250 (1300, N_γ), –290 (2000, N_α); MS (EI) [m/e (¹³⁰Te) (intensity, species)] 230 (11, M⁺ – N₃), 188 (100, M⁺ – 2N₃), 159 (35, C₂H₅Te⁺), 130 (63, Te⁺), 71 (10, C₂H₅N₃⁺), 43 (44, HN₃⁺), 29 (81, C₂H₅⁺). Anal. Calcd for C₄H₁₀N₆Te (269.72): C, 17.8; H, 3.7; N, 31.2. Found: C, 17.2; H, 3.3; N, 29.5.

Properties and Spectral Data for (*n*-C₃H₇)₂Te(N₃)₂ (8). Colorless liquid, yield 91%. IR 2967 m, 2932 m, 2873 m, 2133 m, 2093 s/2067 vs/2023 vs (ν_{as,N_3}), 1524 w, 1488 m, 1458 m, 1406 m, 1383 m, 1314 s, 1258 vs, 1185 m, 1083 m, 1022 m, 956 m, 901 w, 878 w, 815 w, 756 m, 716 m, 649 m, 593 m, 482 w cm⁻¹; Raman 2984 (12), 2966 (12), 2930 (23), 2898 (11), 2078 (7)/2069 (10)/2060 (11)/2026 (6, ν_{as,N_3}), 1311 (5), 1197 (6), 1023 (6), 646 (8), 605 (9), 518 (10)/500 (10, ν_{TeC}), 412 (23), 398 (21), 349 (100, ν_{TeN}), 315 (22), 183 (27), 140 (39), 121 (39) cm⁻¹; ¹H NMR δ 3.04 (CH₂, t, ³J_{H-H} = 7.0 Hz, 4H), 2.02 (CH₂, m, 4H), 1.11 (CH₃, t, 6H); ¹³C NMR δ 40.3 (CH₂Te, ¹J_{C-Te} = 152.2 Hz), 18.8 (CH₂, ²J_{C-Te} = 23.1 Hz), 15.5 (CH₃, ³J_{C-Te} = 30.0 Hz); ¹²⁵Te{¹H} NMR δ 943; ¹⁴N NMR ($\Delta\nu_{1/2}$ [Hz]) δ -137 (60, N _{β}), -246 (620, N _{γ}), -290 (2000, N _{α}); MS (EI) [*m/e* (¹³⁰Te) (intensity, species)] 300 (1, M⁺), 258 (31, M⁺ - N₃), 216 (78, M⁺ - 2N₃), 215 (9, M⁺ - N₃ - C₃H₇), 173 (50, C₃H₇Te⁺), 130 (17, Te⁺), 43 (100, C₃H₇⁺/HN₃⁺), 42 (23, C₃H₆⁺/N₃⁺), 41 (99, C₃H₅⁺). Anal. Calcd for C₆H₁₄N₆Te (297.82): C, 24.2; H, 4.7; N, 28.2. Found: C, 23.3; H, 4.3; N, 28.8.

Properties and Spectral Data for (*i*-C₃H₇)₂Te(N₃)₂ (9). Colorless liquid, yield 91%; IR 2981 m, 2963 m, 2925 m, 2868 m, 2559 w, 2249 w, 2063 vs/2026 vs (ν_{as,N_3}), 1835 w, 1460 s, 1387 m, 1372 m, 1311 m, 1256 m, 1227 m, 1157 m, 1097 w, 1022 m, 912 m, 871 w, 845 m, 735 s, 648 m, 594 m, 497 m, 481 m cm⁻¹; Raman 2968 (22), 2929 (31), 2906 (24), 2874 (13), 2061 (16)/2026 (10, ν_{as,N_3}), 1461 (6), 1444 (6), 1315 (8), 1265 (6), 1212 (12), 1155 (8), 873 (10), 647 (7), 500 (37, ν_{TeC}), 413 (12), 351 (100, ν_{TeN}), 269 (21), 184 (30), 114 (27) cm⁻¹; ¹H NMR δ 3.48 (CH, sept, ³J_{H-H} = 7.0 Hz, ²J_{H-Te} = 41.2 Hz, 2H), 1.73 (CH₃, d, 12H); ¹³C NMR δ 46.7 (CH, ¹J_{C-Te} = 148.0 Hz), 20.8 (CH₃, ²J_{C-Te} = 27.3 Hz); ¹²⁵Te{¹H} NMR δ 1147 (br); ¹⁴N NMR ($\Delta\nu_{1/2}$ [Hz]) δ -136 (40, N _{β}), -207 (70, N _{γ}), -300 (510, N _{α}); MS (EI) [*m/e* (¹³⁰Te) (intensity, species)] 346 (16, M⁺ - 2N₃ + Te), 300 (24, M⁺), 258 (41, M⁺ - N₃), 216 (100, M⁺ - 2N₃), 173 (89, C₃H₇Te⁺), 130 (21, Te⁺). Anal. Calcd for C₆H₁₄N₆Te (297.82): C, 24.2; H, 4.7; N, 28.2. Found: C, 24.3; H, 4.8; N, 26.0.

Properties and Spectral Data for (*c*-C₆H₁₁)₂Te(N₃)₂ (10). Colorless solid, yield 95%, mp 84–86 °C; IR 2934 m, 2918 m, 2852 m, 2559 w, 2509 m, 2063 vs/2021 vs (ν_{as,N_3}), 1443 m, 1337 m, 1313 m, 1251 m, 1175 m, 1103 m, 989 m, 915 w, 885 m, 879 m, 845 w, 801 w, 490 s, 434 m, 420 m cm⁻¹; Raman 2938 (24), 2921 (17), 2895 (8), 2853 (14), 2053 (8)/2023 (15, ν_{as,N_3}), 1461 (5), 1445 (12), 1345 (9), 1330 (6), 1305 (7), 1276 (9), 1263 (12), 1182 (12), 1100 (10), 1023 (11), 990 (8), 882 (5), 846 (10), 803 (8), 660 (28), 492 (7, ν_{TeC}), 422 (5), 355 (100, ν_{TeN}), 333 (15), 236 (15), 204 (30), 168 (14), 120 (20) cm⁻¹; ¹H NMR δ 3.41 (CH, m, 2H), 2.19–1.34 (CH₂, m, 20H); ¹³C NMR δ 55.4 (CH, ¹J_{C-Te} = 160.7 Hz), 30.8 (C₂, ²J_{C-Te} = 19.2 Hz), 28.1 (C₃, ³J_{C-Te} = 23.4 Hz), 25.3 (C₄); ¹²⁵Te{¹H} NMR δ 1117 (br); ¹⁴N NMR ($\Delta\nu_{1/2}$ [Hz]) δ -136 (50, N _{β}), -208 (130, N _{γ}), -300 (850, N _{α}); MS (EI) [*m/e* (¹³⁰Te) (intensity, species)] 426 (16, M⁺ - 2N₃ + Te), 343 (16, C₆H₁₁Te₂⁺), 296 (100, M⁺ - 2N₃), 260 (24, Te₂⁺), 255 (8, C₆H₁₁-TeN₃⁺), 213 (84, C₆H₁₁Te⁺), 130 (8, Te⁺). Anal. Calcd for C₁₂H₂₂N₆Te (377.95): C, 38.1; H, 5.9; N, 22.2. Found: C, 37.9; H, 5.4; N 21.7.

General Procedure for the Preparation of R'Te(N₃)₃ (R' = CH₃, C₂H₅, *n*-C₃H₇, *i*-C₃H₇, C₆H₅, 2,4,6-(CH₃)₃C₆H₂). Into a (red) solution of 1.0 mmol of R'TeTeR' in 10 mL of CH₂Cl₂ at 0 °C was added 3.5 mmol of XeF₂ in small portions. After stirring for 10 min at 0 °C, the solution was stirred for a further 10 min at 25 °C until all XeF₂ disappeared to give clear and colorless solutions. To the solution 8 mmol of Me₃SiN₃ was added slowly. The color changed to yellow and the solution was stirred for a further 40

min. After cooling for 4 h at -18 °C, a colorless to yellowish precipitate of the tellurium(IV) triazides was filtered off and washed with 2 mL of cold CH₂Cl₂. Crystals, which were suitable for X-ray diffraction, were obtained from the washing extracts by cooling to 4 °C.

Properties and Spectral Data for CH₃Te(N₃)₃ (11). Colorless solid, yield 89%, mp 66–67 °C (dec); IR 2097 m/2062 vs/2031 vs (ν_{as,N_3}), 1316 m, 1260 m, 1248 m, 1229 m, 875 w, 853 w, 669 m, 652 m cm⁻¹; Raman 2938 (15), 2128 (3)/2101 (18)/2075 (6)/2051 (7)/2034 (18, ν_{as,N_3}), 1320 (5), 1263 (9), 1252 (4), 1233 (5), 660 (8), 647 (5), 559 (33, ν_{TeC}), 402 (100)/380 (35)/371 (46, ν_{TeN}), 246 (14), 170 (28), 130 (24) cm⁻¹; ¹H NMR (CD₃CN) δ 2.61 (²J_{H-Te} = 30.7 Hz); ¹³C NMR (CD₃CN) δ 29.3; ¹²⁵Te{¹H} NMR (CD₃CN) δ 1405 (br); ¹⁴N NMR (CD₃CN, $\Delta\nu_{1/2}$ [Hz]) δ -137 (30, N _{β}), -244 (200, N _{γ}), -325 (800, N _{α}); MS (EI) [*m/e* (¹³⁰Te) (intensity, species)] 271 (3, M⁺), 229 (58, M⁺ - N₃), 187 (30, M⁺ - 2N₃), 145 (26, M⁺ - 3N₃), 130 (18, Te⁺), 43 (34, HN₃⁺), 42 (32, N₃⁺), 28 (100, N₂⁺).

Properties and Spectral Data for C₂H₅Te(N₃)₃ (12). Colorless crystals, yield 43%, mp 85–87 °C (dec); IR 3285 w, 2725 w, 2566 w, 2466 vw, 2442 w, 2122 m/2097 s/2068 vs/2045 vs/2030 vs (ν_{as,N_3}), 1443 s, 1407 w, 1338 w, 1309 s, 1264 m, 1242 m, 1229 s, 1214 s, 1168 m, 1033 m, 996 m, 956 m, 728 s, 664 s, 648 s, 590 s, 559 w, 499 m (ν_{TeC}), 408 s cm⁻¹; Raman 3002 (3), 2984 (7), 2939 (12), 2925 (12), 2863 (3), 2114 (33)/2060 (15)/2041 (21)/2035 (16, ν_{as,N_3}), 1441 (4), 1408 (3), 1372 (2), 1314 (6), 1263 (4), 1247 (7), 1230 (7), 1215 (7), 1036 (2), 1000 (3), 958 (2), 667 (10), 650 (9), 499 (28, ν_{TeC}), 441 (7), 406 (100)/369 (31)/345 (73, ν_{TeN}), 300 (15), 268 (17), 254 (26), 183 (52), 128 (60) cm⁻¹; ¹H NMR δ 3.30 (CH₂, q, ³J_{H-H} = 7.7 Hz, 2H), 1.82 (CH₃, t, ³J_{H-Te} = 36.1 Hz, 3H); ¹³C NMR δ 42.1 (CH₂), 8.8 (CH₃); ¹²⁵Te{¹H} NMR δ 1363; ¹⁴N NMR ($\Delta\nu_{1/2}$ [Hz]) δ -140 (30, N _{β}), -243 (1400, N _{γ}); MS (EI) [*m/e* (¹³⁰Te) (intensity, species)] 285 (2, M⁺), 243 (14, M⁺ - N₃), 201 (37, M⁺ - 2N₃), 159 (30, M⁺ - 3N₃), 130 (41, Te⁺), 43 (59, HN₃⁺), 29 (77, C₂H₅⁺), 28 (100, C₂H₄⁺/N₂⁺).

Properties and Spectral Data for *n*-C₃H₇Te(N₃)₃ (13). Colorless crystals, yield 60%, mp 84–87 °C (dec); IR 2726 w, 2675 vw, 2439 w, 2130 m/2090 s/2041 vs/2028 vs (ν_{as,N_3}), 1308 s, 1262 m, 1243 m, 1227 s, 1149 w, 1077 m, 1017 w, 721 s, 664 m, 649 s, 591 m, 405 s cm⁻¹; Raman 2986 (5), 2938 (10), 2930 (10), 2876 (3), 2112 (30)/2059 (10)/2043 (27, ν_{as,N_3}), 1453 (3), 1315 (6), 1259 (4), 1249 (6), 1228 (6), 1194 (7), 1021 (7), 666 (11), 653 (7), 596 (11), 441 (8), 405 (100)/367 (35)/350 (70, ν_{TeN}), 288 (17), 251 (23), 179 (43), 142 (32) cm⁻¹; ¹H NMR δ 3.25 (CH₂, t, ³J_{H-H} = 7.8 Hz, 2H), 2.15 (CH₂, m, 2H), 1.17 (CH₃, t, 3H); ¹³C NMR δ 49.8 (CH₂-Te, ¹J_{C-Te} = 188.0 Hz), 17.9 (CH₂), 15.8 (CH₃); ¹²⁵Te{¹H} NMR δ 1378 (br); ¹⁴N NMR ($\Delta\nu_{1/2}$ [Hz]) δ -140 (60, N _{β}), -238 (600, N _{γ}); MS (EI) [*m/e* (¹³⁰Te) (intensity, species)] 257 (10, M⁺ - N₃), 215 (95, M⁺ - 2N₃), 173 (60, M⁺ - 3N₃), 130 (11, Te⁺), 43 (100, C₃H₇⁺/HN₃⁺), 42 (60, C₃H₆⁺/N₃⁺).

Properties and Spectral Data for *i*-C₃H₇Te(N₃)₃ (14). Colorless crystals, yield 38%, mp 108–109 °C (dec); IR 3298 w, 2949 vs, 2939 vs, 2923 w, 2907 vs, 2130 s/2095 s/2055 s/2032 s (ν_{as,N_3}), 1366 w, 1312 m, 1260 m, 1237 m, 1216 m, 1149 m, 1099 w, 1025 m, 932 w, 865 w, 650 m, 585 w, 495 w (ν_{TeC}), 417 m, 353 vw, 348 vw, 329 vw, 308 m, 305 m cm⁻¹; Raman 3071 (5), 2968 (12), 2954 (7), 2927 (14), 2117 (20)/2095 (26)/2071 (30)/2042 (16, ν_{as,N_3}), 1327 (15), 1267 (14), 1219 (15), 651 (23), 496 (25, ν_{TeC}), 423 (80)/415 (100)/343 (85, ν_{TeN}), 306 (36), 289 (35), 241 (25), 215 (25), 193 (26), 124 (40), 106 (42), 87 (37) cm⁻¹; ¹H NMR δ 3.76 (CH, sept, ³J_{H-H} = 7.0 Hz, 1H), 1.79 (CH₃, d, 6H); ¹³C NMR δ 56.3 (CH, ¹J_{C-Te} = 170.3 Hz), 18.7 (CH₃); ¹²⁵Te{¹H} NMR δ 1399; ¹⁴N NMR ($\Delta\nu_{1/2}$ [Hz]) δ -140 (30, N _{β}), -240 (430, N _{γ}); MS (EI)

[*m/e* (¹³⁰Te) (intensity, species)] 299 (4, M⁺), 257 (54, M⁺ – N₃), 215 (38, M⁺ – 2N₃), 130 (30, Te⁺), 43 (100, C₃H₇⁺/HN₃⁺), 42 (32, C₃H₆⁺/N₃⁺).

Properties and Spectral Data for C₆H₅Te(N₃)₃ (15). Colorless solid, yield 40%, mp 117–118 °C (dec); IR 3299 vw, 3053 w, 2725 vw, 2131 m/2033 vs (ν_{as,N_3}), 1574 w, 1437 s, 1309 m, 1254 m, 1181 w, 1158 w, 1091 vw, 1059 m, 1019 w, 997 w, 919 vw, 891 vw, 845 vw, 801 vw, 735 s, 686 s, 645 m, 459 m cm⁻¹; Raman 3062 (15), 2111 (24)/2094 (12)/2063 (14)/2040 (13, ν_{as,N_3}), 1575 (7), 1317 (7), 1289 (9), 1248 (11), 1019 (13), 996 (20), 660 (11), 652 (22), 410 (100)/355 (59)/339 (80, ν_{TeN}), 275 (26), 246 (23), 199 (32), 143 (34), 118 (34), 84 (58) cm⁻¹; ¹H NMR δ 7.96–7.67 (m); ¹³C NMR δ 136.2 (C1, br), 133.6 (C2), 131.7 (C3), 130.8 (C4); ¹²⁵Te{¹H} NMR δ 1284 (br); ¹⁴N NMR ($\Delta\nu_{1/2}$ [Hz]) δ –139 (40, N_β), –228 (2000, N_γ); MS (EI) [*m/e* (¹³⁰Te) (intensity, species)] 284 (60, (C₆H₅)₂Te⁺), 207 (23, C₆H₅Te⁺), 154 (100, (C₆H₅)₂⁺), 130 (3, Te⁺), 77 (97, C₆H₅⁺), 51 (48, C₄H₃⁺).

Properties and Spectral Data for 2,4,6-(CH₃)₃C₆H₂Te(N₃)₃ (16). Pale yellow crystals, yield 58%, mp 148–149 °C (dec); IR 3277 vw, 2867 vs, 2726 vw, 2131 w/2089 m/2061 s/2049 s (ν_{as,N_3}), 1591 vw, 1557 vw, 1292 m, 1247 m, 1223 m, 1168 w, 1150 w, 1028 vw, 922 vw, 856 m, 772 vw, 722 m, 696 vw, 655 w, 647 w, 590 w, 576 w, 561 vw, 543 m, 527 w, 500 vw, 412 m cm⁻¹; Raman 3031 (8), 2992 (8), 2980 (8), 2961 (6), 2928 (13), 2908 (9), 2868

(4), 2089 (29)/2071 (11)/2042 (28, ν_{as,N_3}), 1594 (8), 1565 (3), 1466 (3), 1444 (5), 1388 (11), 1379 (6), 1311 (6), 1294 (13), 1277 (4), 1257 (6), 1179 (2), 1037 (2), 1003 (4), 949 (2), 647 (14), 581 (7), 555 (20), 529 (9), 407 (100)/354 (54)/339 (93, ν_{TeN}), 250 (22), 236 (14), 183 (37), 161 (37), 119 (40) cm⁻¹; ¹H NMR (CD₂Cl₂) δ 7.07 (CH, br, 2H), 2.67 (*o*-CH₃, s, 6H), 2.33 (*p*-CH₃, s, 3H); ¹³C NMR (CD₂Cl₂) δ 143.7 (C4), 143.0/139.2 (C2, br), 132.6/130.8 (C3, br), 133.2/131.9 (C1, br), 22.8/20.4 (*o*-CH₃, br), 21.0 (*p*-CH₃); ¹²⁵Te-{¹H} NMR (CD₂Cl₂) δ 1252; ¹⁴N NMR (CD₂Cl₂, $\Delta\nu_{1/2}$ [Hz]) δ –141 (70, N_β), –189 (140, N_γ), –292 (400, N_α); MS (EI) [*m/e* (¹³⁰Te) (intensity, species)] 498 (11, (C₉H₁₁)₂Te₂⁺), 333 (1, C₉H₁₁-Te(N₃)₂⁺), 291 (5, C₉H₁₁TeN₃⁺), 249 (10, C₉H₁₁Te⁺), 119 (100, C₉H₁₁⁺), 43 (28, HN₃⁺).

Acknowledgment. The University of Munich and the Fonds der Chemischen Industrie are gratefully acknowledged for financial support.

Supporting Information Available: Crystallographic files in CIF format for compounds **12**, **13**, **14**, and **16**; Raman spectrum of CH₃Te(N₃)₃ (**11**) and polymer structure of *n*-C₃H₇Te(N₃)₃ (**13**), Figure 2b. This material is available free of charge via the Internet at <http://pubs.acs.org>.

IC011026+